RELATIVE NAVIGATION TO NON-COOPERATIVE TARGETS IN LEO: ACHIEVABLE ACCURACY FROM RADAR TRACKING MEASUREMENTS

Ralph Kahle[(1)]**, Martin Weigel**[(2)]**, Michael Kirschner,**[(3)] **Sofya Spiridonova**[(4)]**, Erin Kahr**[(5)] **and Klemens Letsch**[(6)]

[(1-4)]*German Aerospace Center (DLR), German Space Operations Center (GSOC), Oberpfaffenhofen, 82234 Wessling, Germany, +49-8153-282451,* [*ralph.kahle@dlr.de*](ralph.kahle@dlr.de)
[(5)]*Department of Geomatics Engineering, Schulich School of Engineering, University of Calgary, Canada,* [*erinkahr@hotmail.com*](erinkahr@hotmail.com)
[(6)]*Fraunhofer Institute for High Frequency Physics and Radar Techniques (FHR), Neuenahrer Str. 20, 53343 Wachtberg, Germany,* [*klemens.letsch@fhr.fraunhofer.de*](klemens.letsch@fhr.fraunhofer.de)

Abstract: *Any future space debris removal or on-orbit servicing mission faces the problem of the initial relative orbit determination of the servicing satellite to the non-cooperative target. In this work we analyze the relative navigation accuracy that can be achieved in low Earth orbit, by using ground-based orbit determination from radar tracking measurements for the target, and classical GPS-based orbit determination for the servicing satellite. The analysis is based on the radar tracking measurements obtained from a 10x10x34 cm small object at an altitude of 635 km. The results show that the relative orbit can be determined with accuracy down to 2 m (RMS) in the semi-major axis, and down to 20 m (RMS) in both the radial and normal separations. From the results we derive requirements on radar-tracking campaigns.*

Keywords: *Relative Navigation, Radar Tracking, On-Orbit Servicing, Space Debris Removal*

1. Introduction

This work focuses on the relative navigation accuracy achievable for the approach of a servicing satellite to a non-cooperative target in low Earth orbit. Such a scenario might be encountered by space debris removal or on-orbit servicing missions with lacking positioning capability of the target. As a general mission objective the active spacecraft (in the following called Servicer) must be maneuvered to a desired initial formation with the non-cooperative target, i.e. an un-controlled piece of debris or a satellite (Client). Depending on the available on-board sensors for relative navigation the required along-track separation of the initial formation will be on the order of 1 km to 100 km. At this distance the rendezvous payload on-board the Servicer can take over the task of relative navigation in order to (autonomously) rendezvous and finally catch or dock the Client.

In general, the Servicer orbit will be known to either centimeter accuracy from precise orbit determination utilizing GPS receiver pseudo-range and carrier phase measurements, or to meter level accuracy when filtering the GPS navigation solution data. On the contrary, the Client orbit will only be known to kilometer level accuracy when relying on TLE data from USSTRATCOM. Clearly, the Client orbit knowledge drives the achievable relative orbit knowledge and thus should be determined as

precisely as possible too. In this paper we focus on the refinement of the TLE-based orbit of the non-cooperative Client by using measurements from a dedicated ground radar tracking campaign.

In order to quantify the orbit accuracy achievable for the Client and furthermore the accuracy of the Servicer-Client relative orbit, an extensive radar tracking campaign was conducted in early 2012 [1]. The Tracking and Imaging Radar (TIRA) of Fraunhofer FHR in Wachtberg, Germany, was used to track the Canadian nano-satellite CanX-2 over a period of five days. CanX-2 is a triple CubeSat of the size 10x10x34 cm carrying a dual frequency GPS receiver [2]. Because of its orbital features (635 km altitude, sun-synchronous polar orbit), its small size, and because it provides accurate reference orbit data we consider CanX-2 as a perfect candidate for demonstrating the ground relative navigation concept.

In our previous work [1] we established a reference trajectory using precise orbit determination with CanX-2's GPS measurements. The orbital information derived from radar-tracking measurements was than compared against the reference orbit to obtain statistics of the position determination and prediction accuracies for different radar tracking arc lengths and for different numbers of tracking passes. In this work, we implemented a new TIRA data pre-processing, which removes bad range and angle measurement based on the evaluation of the radar signal amplitude. We then apply the statistical orbit determination accuracy analysis as described in [1] to the 529 tracking cases. We next determine the accuracies of the ballistic coefficient and the mean orbit elements rather than position accuracies. Knowing the corresponding accuracies for GPS-based orbit determination of the Servicer, we finally derive the achievable accuracy of the Servicer-Client relative orbital elements. The paper concludes with a discussion on the radar tracking requirements.
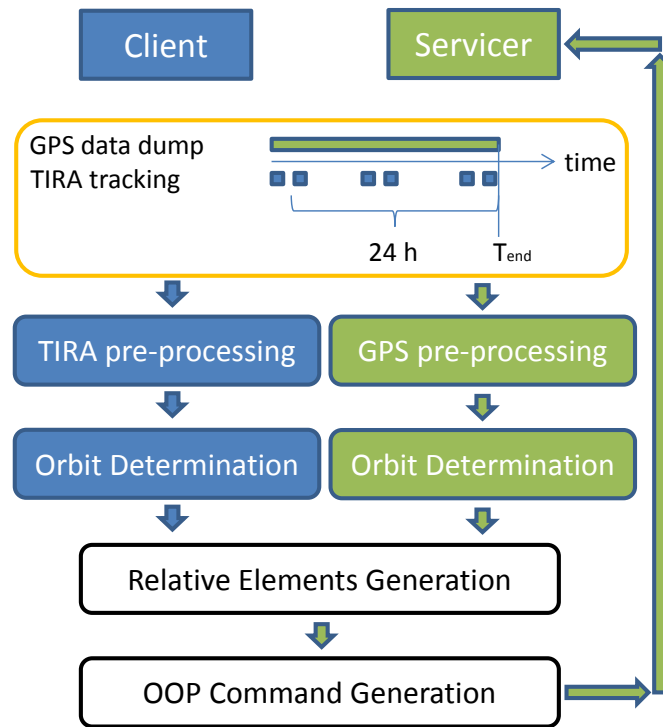
2. Far-Range Navigation Concept

In general, the far range approach of the servicing satellite to the Client will be based on absolute orbit determination carried out on the ground [3]. For the case of the Servicer we consider the orbit determination process to be based on Servicer GPS raw or navigation solution data. Contrarily, the initial orbit of the Client will be provided by means of TLE data which can be refined by determining the orbit from radar tracking measurements of the Client.

The far range navigation concept is illustrated in Fig. 1. Both the Client and Servicer spacecraft are presented at the top. The Servicer housekeeping telemetry including the GPS navigation data is downlinked over the prime ground-station, e.g. Weilheim in Germany. The Client is considered to be entirely non-cooperative and TIRA radar tracking is performed for the Client. Because of the TIRA location in Wachtberg (near Bonn, Germany) the TIRA and Weilheim passes take place almost at once. The corresponding measurement timeline is shown in the orange box. While Servicer GPS dump data is available without gaps, Client radar tracking measurements are only available at the moment of TIRA passes. Typically, 4-5 TIRA passes (with elevation >

10 deg) can be conducted within approx. 24 hours for a polar 400 km altitude orbit. For higher polar orbits, e.g. at 550 km altitude, up to 6 TIRA tracking passes can be performed in the same period.

Both the TIRA measurements and the GPS dump data are transferred from the ground-stations to the Servicer control center for further processing, i.e. data pre-processing and absolute orbit determination. Then, the Servicer-Client relative orbital elements (ROE) are determined, and a Servicer on-board orbit propagator (OOP) command file is generated. After the OOP is uploaded to the Servicer, on-board relative motion propagation can be performed. Regular OOP updates can be provided from the ground every 12 or 24 hours depending on the availability of further Client radar measurements.

Figure 1. Navigation concept for the far range approach.

Based on the relative orbital elements, the far formation can then be maneuvered into a closer one, either on-board autonomously based on the OOP, or by ground-in-the-loop. At this point the rendezvous payload on-board the Servicer can take over the tasks of relative navigation in order to autonomously (or ground-augmented) rendezvous and finally catch or dock the Client. For example, this could occur from a 30 km distance by means of optical navigation as demonstrated with the PRISMA mission [4].

3. Orbit Determination from Radar Tracking

In order to quantify the orbit accuracy achievable for the Client and furthermore the accuracy of the Servicer-Client relative orbit, an extensive radar tracking campaign was

conducted in the period from Feb. 27 to Mar. 2, 2012. In this section we describe the campaign, the data processing and the obtained results.

3.1 CanX-2 Tracking Campaign

CanX-2 is a triple CubeSat with dimensions 10 x 10 x 34 cm. It was built under the Canadian Advanced Nanospace eXperiment (CanX) program and is operated by the University of Toronto Institute for Aerospace Studies, Space Flight Laboratory (UTIAS/SFL) [2]. CanX-2 is orbiting the Earth in a Sun-synchronous polar orbit with a 635km altitude and a 9:30 am descending node. Due to the nanosatellite's power, data storage volume and downlink constraints the GPS receiver was only operated for approximately 90 minutes twice daily. The GPS on-time was coordinated with the visibility of CanX-2 for TIRA. Synchronization or even simultaneity of observations ensures radar measurement evaluation at the times with the most precise GPS position information. The cold gas propulsion subsystem was not activated throughout the campaign and, therefore, orbit maneuvers do not have to be taken into account. The size of CanX-2 and the provision of accurate reference orbit data make CanX-2 a desirable test target for orbit determination of 'space debris'.

TIRA's location at 50.6° northern latitude and the sun-synchronous dusk-dawn orbit of CanX-2 lead to a regular visibility pattern of 2 to 3 station passes in the morning and evening of each day. Operation time constraints were incorporated into the radar tracking planning. Out of the morning group of station passes the two passes with the highest elevation were selected for radar tracking, as well as 1 or 2 station passes in the evening of every second day. This observation schedule resulted in a total of 14 station passes to be tracked within the 5-day campaign.

3.2 CanX-2 Reference Orbit

The precise orbit generated from processing CanX-2's GPS data is used as a reference for the radar measurement results. CanX-2 carries a NovAtel OEM4-G2L dual frequency GPS receiver, which provides L1 C/A tracking and semi-codeless L2 P(Y) tracking [5]. Besides GPS navigation fixes the receiver delivers pseudo-range and carrier phase measurements. To allow for precise orbit determination on-ground the GPS raw observations are part of the downlink telemetry alongside the nanosatellite's attitude information.

The precise orbit was determined with the DLR/GSOC Reduced Dynamics Orbit Determination software using GPS pseudo-range and carrier phase measurements as input. The estimated reference orbit accuracy is 1 m (RMS) in the radial and cross-track components and 5 m in the along-track component during periods when the receiver was turned on [1]. Thus, the reference orbit is well suited for the following radar tracking assessment.

3.3 TIRA Data Pre-Processing

As discussed in [1] the measurement quality obtained from the radar tracking of the small object was significantly degraded as compared to tracking of meter-level objects. A closer look into the TIRA measurement data shows a correlation between the amplitude [dB] and the measurement errors. The bad measurements or outliers can easily be detected and rejected from an evaluation of the amplitude distribution over each tracking pass.

The measurement quality is evaluated based on the mean and standard deviation of the signal amplitude over each tracking pass. The measurements acquired with a signal amplitude less than Mean(amplitude) - 0.6*Std(amplitude) are considered to be of inferior quality and are discarded before running the orbit determination process. This simple procedure eliminates on average the "worst" 35% of the measurement data.
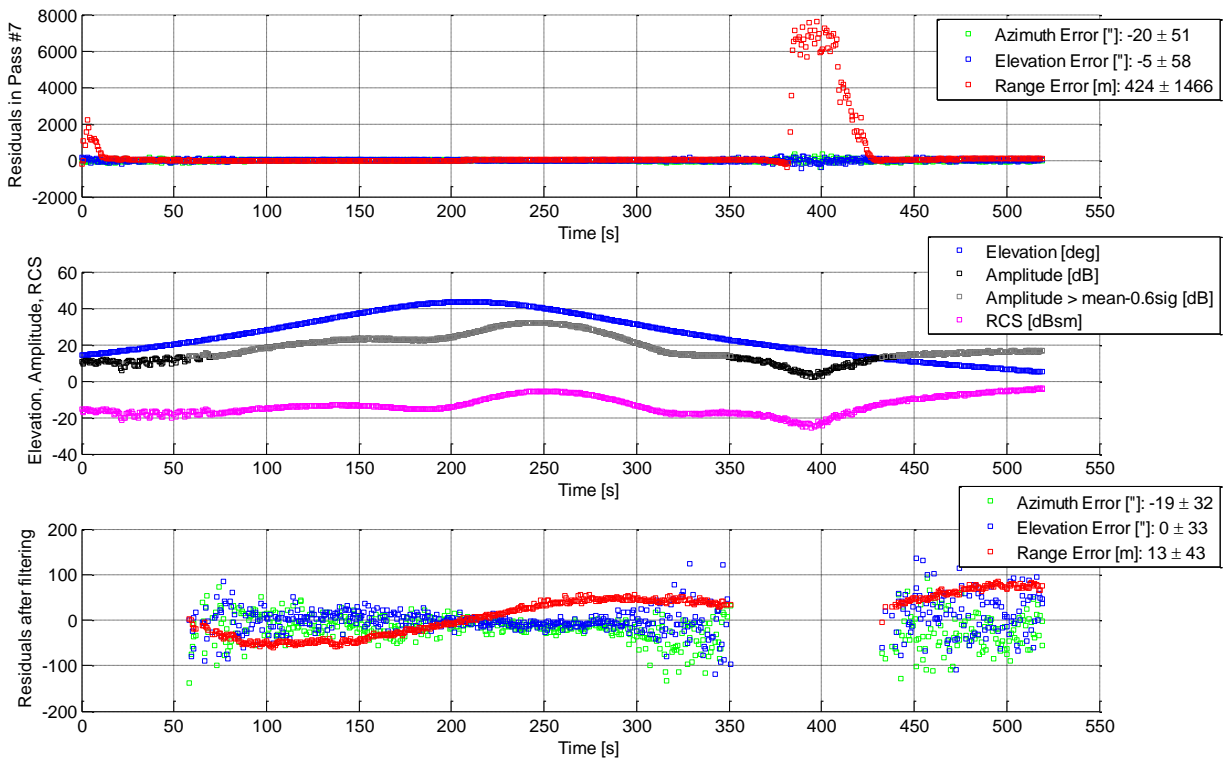
Figure 2. Example pre-processing of CanX-2 pass #7. Top: TIRA measurement residuals before pre-processing. Middle: elevation, amplitude, and radar cross section (RCS). Bottom: Residuals after filtering.

Results are shown for one selected tracking pass in Fig. 2. In the top subplot, the residuals of the TIRA measurements as compared to the results of the GPS-based Precise Orbit Determination are plotted. Here we can observe some very large outliers, in particular in the range component (in red). Clearly, the areas of large outliers correspond to the lows in the amplitude of the signal, pictured in grey/black in the middle subplot. For completeness, the elevation is depicted in blue (middle subplot), and the radar cross section (RCS) in pink, a parameter derivable from amplitude. The

areas of amplitude lower than the selected threshold are marked with black in the middle subplot. Most of the prominent outliers could be detected and eliminated before the orbit determination process (bottom subplot). As a result a significant improvement in the orbit determination accuracy, especially the elements RAAN and inclination, was achieved compared to [1].

3.4 Statistical Orbit Determination Accuracy Analysis

Out of all 14 tracking passes smaller data sets are selected to construct multiple cases of identical tracking scenarios. A tracking scenario is characterized by a principal tracking duration and the number of tracking passes used. The term principle tracking duration reflects the presence of two groups of station passes every day for polar orbiting satellites. The principle tracking duration is always a multiple of 12 hours as the groups of station passes on the ascending and descending arc are separated by half of the Earth rotation time. The selection of 2-8 tracking passes from the full data set results in a total number of 529 orbit determination (OD) cases with a maximum principle tracking duration of 48 hours.

Care has to be taken when building the scenarios with 24h and 48h principle tracking durations. Here, ascending and descending measurements can be combined or exclusively processed. The two types of combinations are analyzed separately for the 24h and 48h scenarios. Scenarios that are exclusively based on ascending or descending passes are labeled with a star * in the following figures. For cases having a principal tracking duration of 0h (i.e. all observations are taken in subsequent orbits) only ascending passes or descending passes are involved. By definition an arbitrary selection of station passes within a principal tracking duration of 12 h and 36 h will always be a combination of ascending and descending passes.

Multiple cases with comparable tracking durations and identical numbers of station passes can be selected. Beyond comparing single OD cases with the reference orbit it is therefore possible to derive statistical quantities on the achievable orbit determination accuracy for each tracking scenario.

3.5 Client Orbit Determination Results

The setup and processing of orbit determination results from radar-tracking measurements is described in [1]. The processing is repeated with the filtered TIRA measurements. Again, a convergent solution is obtained in all 529 OD cases. For each solution the osculating Kepler elements are then transformed into mean orbital elements (MOE) by subtracting the dominating short-period perturbations due to J2. The MOE for each OD case is compared against the reference orbit and the differences in the mean orbital elements are computed.

Because of the chosen concept we are only interested in the errors at the end of a radar tracking arc (i.e. T_{end} in Fig. 1). The relative orbit elements at this epoch can then be determined from the state of the Client and the corresponding state of the Servicer. Fig.

3, 5, and 6 depict the errors in the mean orbital elements for each OD case for the semi-major axis, inclination and RAAN, respectively. In addition, the relative error of the ballistic coefficient compared to a ballistic coefficient estimated from the GPS POD trajectory is presented in Fig. 4.
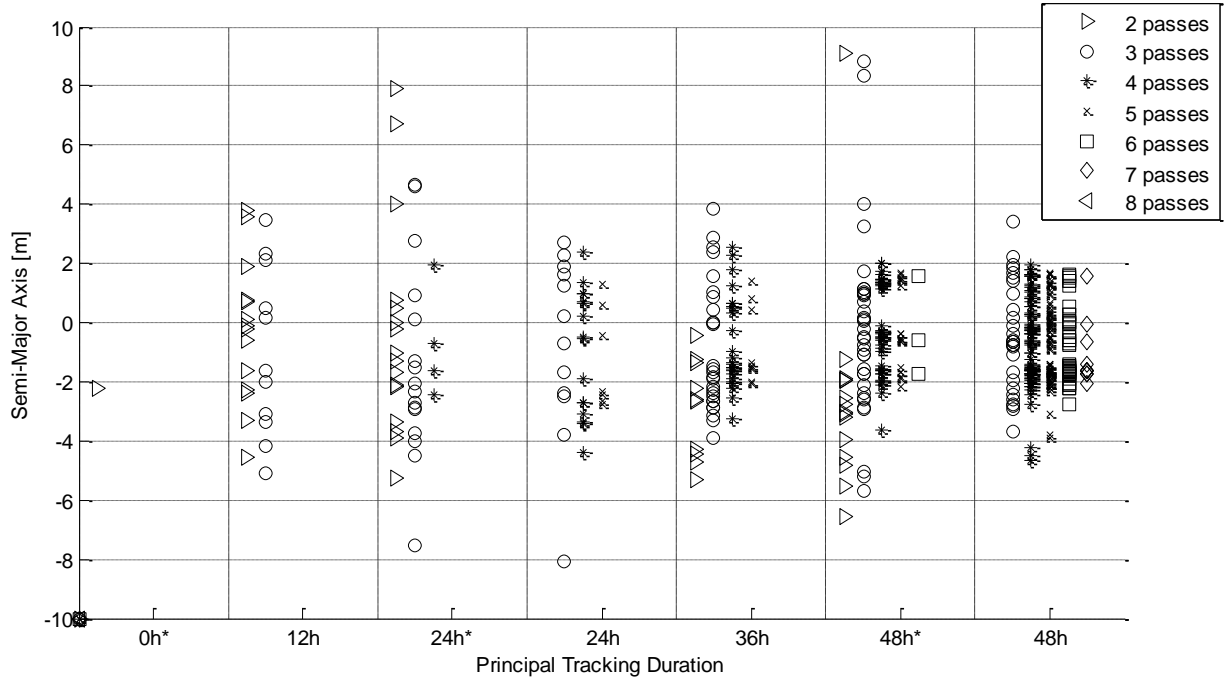
Figure 3. Semi-major axis error at observation arc end as a function of principal tracking duration and tracking pass number. Exclusive combinations of ascending or descending observations are indicated by a * in the x axis label.
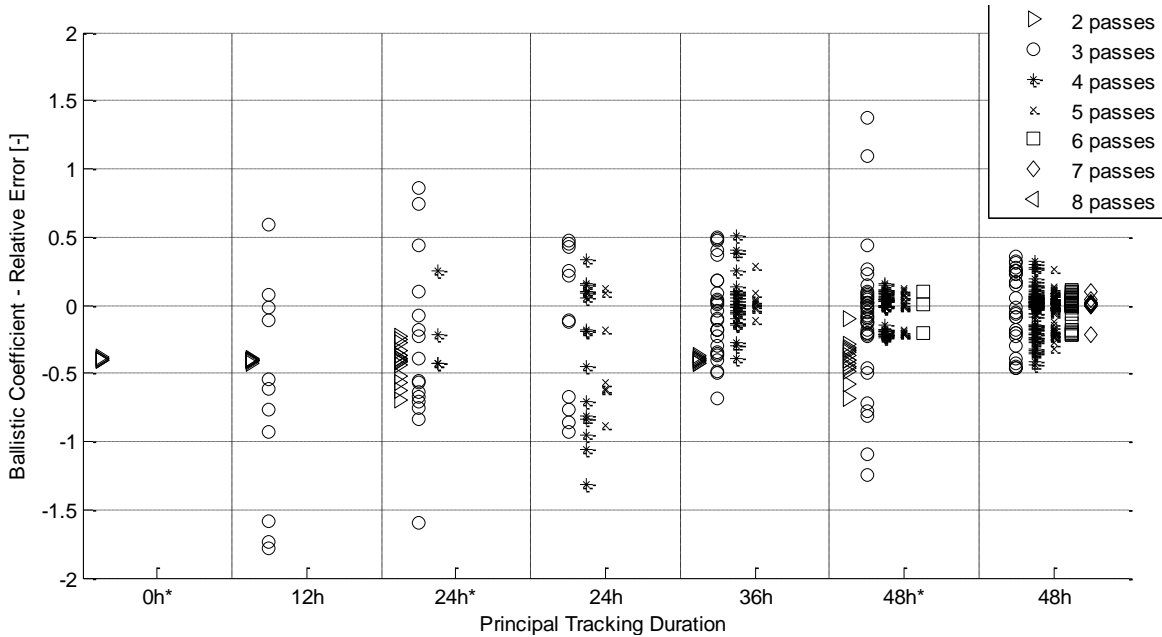
Figure 4. Relative error in the Ballistic Coefficient as a function of principal tracking duration and tracking pass number. Exclusive combinations of ascending or descending observations are indicated by a * in the x axis label.
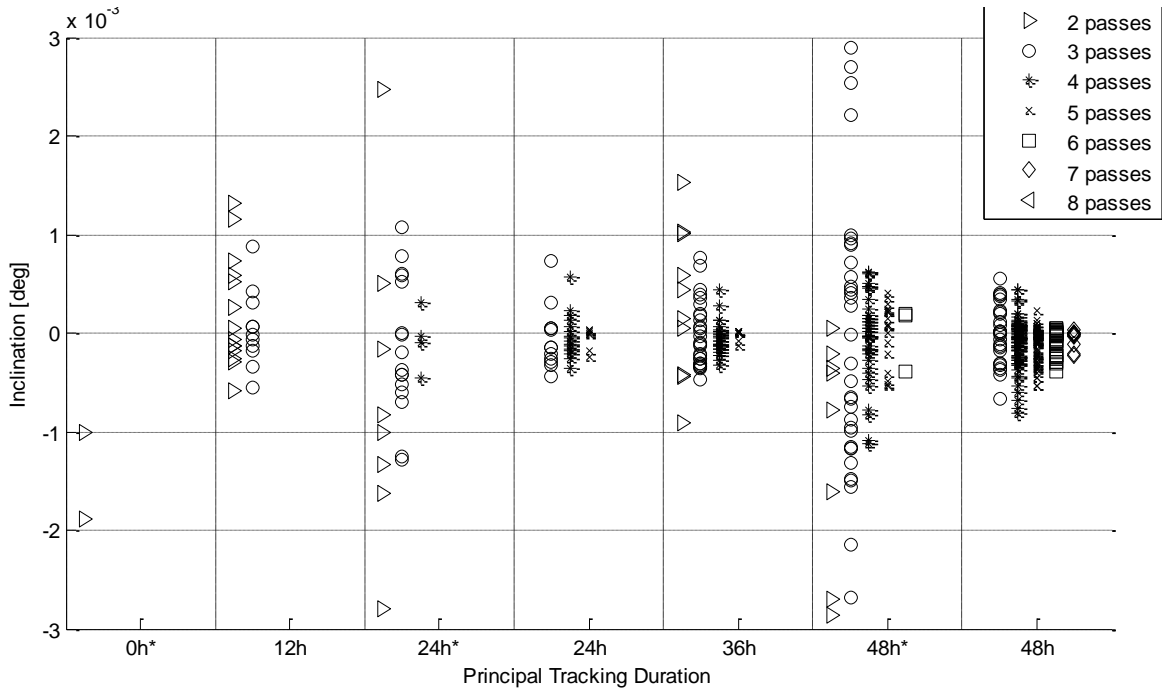
Figure 5. Inclination error at observation arc end as a function of principal tracking duration and pass number. Exclusive combinations of ascending or descending observations are indicated by a * in the x axis label.
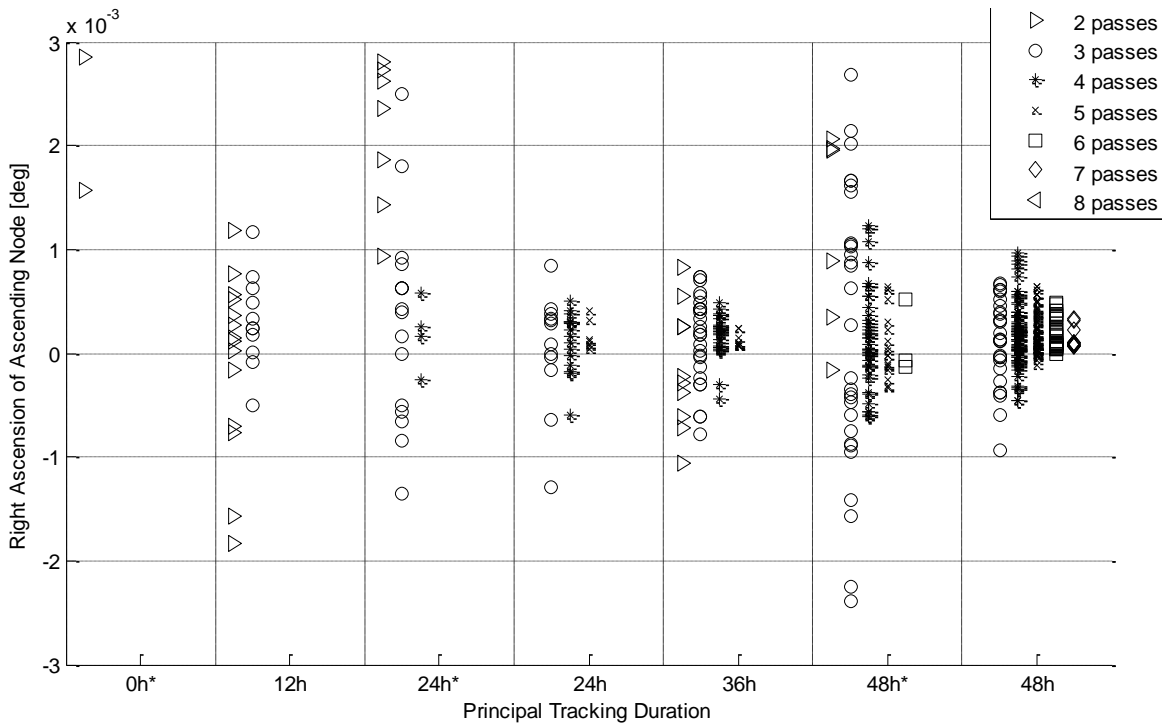

Figure 6. RAAN error at observation arc end as a function of principal tracking duration and pass number. Exclusive combinations of ascending or descending observations are indicated by a * in the x axis label.

Clearly, tracking scenarios that include mixed combinations of ascending and descending orbital arcs lead to much smaller orbital element errors than similar scenarios that are exclusively based on ascending or descending observations (i.e. 0h*, 24h*, and 48h* in Fig. 5 and 6). Mixed combinations imply observations taken from opposite sides of the orbit. The more diverse tracking geometry facilitates a better orbit determination and hence a higher accuracy. With increasing tracking arc length and increasing number of passes the ballistic coefficient is determined more accurately.

From the individual MOE errors at the end of an observation arc we compute the mean and standard deviations for each tracking scenario (i.e. groups of similar OD cases). Each tracking scenario comprises OD cases with equal principal tracking duration and equal number of tracking passes. Note that scenarios with less than 3 OD cases are not evaluated. In Tab. 1 the RMS values quantifying the accuracy of each of the six mean orbital elements and the relative error of the ballistic coefficient are summarized for the favorable tracking scenarios using the following abbreviations:

PTD   Principal Tracking Duration
NTP   Number of Tracking Passes
Number of orbit determination cases
a Semi-major axis
e Eccentricity
i Inclination
Ω Right Ascension of the Ascending Node
ω Argument of Perigee
$u = \omega + M$ Argument of Latitude
B Ballistic Coefficient.

Table 1. RMS values for the mean orbital elements and relative error in the ballistic coefficient for favorable tracking scenarios.

PTD, NTP	#	a [m]	e [-]	i [deg]	Ω [deg]	ω [deg]	u [deg]	B [%]
24h, 3	12	3.23	5.17E-6	3.25E-4	5.58E-4	1.51E-1	8.54E-4	86.24
24h, 4	16	2.31	4.93E-6	2.24E-4	3.10E-4	8.04E-2	6.39E-4	62.95
24h, 5	7	2.11	5.05E-6	1.20E-4	2.19E-4	7.29E-2	5.85E-4	54.29
36h, 3	27	2.33	6.24E-6	3.32E-4	4.48E-4	1.50E-1	7.39E-4	33.00
36h, 4	25	1.70	4.14E-6	1.73E-4	2.77E-4	7.31E-2	4.77E-4	21.06
36h, 5	9	1.54	3.04E-6	5.73E-5	1.45E-4	3.51E-2	2.97E-4	11.49
48h, 3	28	1.91	4.82E-6	3.02E-4	4.27E-4	1.38E-1	7.66E-4	27.34
48h, 4	74	1.65	3.36E-6	2.58E-4	3.64E-4	7.95E-2	5.08E-4	16.65
48h, 5	82	1.53	2.40E-6	1.89E-4	2.77E-4	5.89E-2	4.30E-4	11.40
48h, 6	44	1.50	1.73E-6	1.42E-4	2.22E-4	5.15E-2	3.74E-4	8.97
48h, 7	11	1.56	1.40E-6	1.03E-4	1.75E-4	4.68E-2	3.42E-4	7.50

Of the 27 tracking scenarios presented in [1], only 11 have been considered in this analysis. The tracking scenarios with less than 3 tracking passes, a principal tracking duration of 12 hours or less, and those with tracking performed either only in the

ascending or only in the descending part of the orbit have been discarded as inferior and therefore inadvisable.

3.6 Servicer Orbit Determination Characteristic

GPS-based OD errors have been investigated in a manner comparable to the one for TIRA OD. Typical TerraSAR-X orbit determination from GPS navigation data has been evaluated in comparison with the highly accurate results of precise orbit determination (e.g. [6]). Mean offsets and standard deviations for nine sample days have been selected to derive the statistical quantities. The RMS errors of the mean orbital elements are summarized in Tab. 2.

Table 2. Typical RMS errors for GPS navigation based orbit determination.

	a [m]	e [-]	i [deg]	Ω [deg]	ω [deg]	u [deg]
RMS	0.37	4.5E-8	1.2E-5	3.1E-6	1.8E-3	3.1E-5

4. Expected Servicer-Client Relative Orbital Elements Accuracy

In sections 3.5 and 3.6, the absolute orbital element errors for the orbit determination based on radar-tracking measurements and GPS navigation solutions were discussed. The current section finally addresses the question of errors in the Servicer-Client relative orbital elements (ROE). We apply the following convention for calculating the relative orbital elements (ROE) from the servicer and client MOE [7]:

$$
\begin{pmatrix} \delta a \\ a\delta\lambda \\ a\delta e_x \\ a\delta e_y \\ a\delta i_x \\ a\delta i_y \end{pmatrix} = \begin{pmatrix} a - a_c \\ a(u - u_c) + a(\Omega - \Omega_c)\cos i \\ a(e_x - e_x^c) \\ a(e_y - e_y^c) \\ a(i - i_c) \\ a(\Omega - \Omega_c)\sin i \end{pmatrix}.
\tag{1}
$$

Here, the mean orbital elements $(a, u, e_x, e_y, i, \Omega)$ parameterize the absolute orbit of the Servicer spacecraft, with

$$
\begin{pmatrix} e_x \\ e_y \end{pmatrix} = \begin{pmatrix} e\cos\omega \\ e\sin\omega \end{pmatrix}
$$
being the eccentricity vector.

The same symbols with additional index c refer to the mean orbital elements of the Client satellite. The relative orbital elements are the relative semi-major axis δa, the relative mean longitude $a\delta\lambda$, the relative eccentricity vector $a\delta\vec{e}$, and the relative inclination vector $a\delta\vec{i}$.

In the likely case of differences in the ballistic coefficients of the Servicer and the Client a differential air drag is exerted on the formation. The following equation applied to model the influence of the atmospheric drag on the relative orbital elements over time [7]:

$$
\begin{pmatrix} \delta\delta a \\ a\delta\delta\lambda \\ a\delta\delta e_x \\ a\delta\delta e_y \\ a\delta\delta i_x \\ a\delta\delta i_y \end{pmatrix}_{Drag} = \begin{pmatrix} -\frac{1}{n}\Delta B\rho v^2(t-T_{End}) \\ +\frac{3}{4}\Delta B\rho v^2(t-T_{End})^2 \\ 0 \\ 0 \\ 0 \\ 0 \end{pmatrix}, \tag{2}
$$

where n is the mean motion, $\Delta B = C_D(\frac{A_s}{m_s} - \frac{A_c}{m_c})$ is the relative ballistic coefficient, C_D is the aerodynamic drag coefficient, A is the satellite cross-section area, m is the satellite mass, ρ is the atmospheric density, and v is the satellite velocity.

Adding the drag term (Eq. 2) to the relative orbital elements at time T_{end} (Eq. 1) then yields the relative orbital elements at a future time t, e.g. the moment of on-board orbit propagator initialization. For a discussion of other ROE influences like J2 perturbation or maneuver handling please refer to [7].

In the following we derive the relative orbital element errors for an example mission with the following orbit characteristics: a = 6928.137 km (i.e. 550 km altitude), e = 0.002, i = 87.0 deg. We set the Client ballistic coefficient to 0.0069 m²/kg (e.g. C_D = 2.3, A = 3 m², m = 1000 kg) and consider a mean density ρ = 2.21E-13 kg/m³. The radar tracking RMS errors for the client spacecraft are assumed to be the same as those presented in Tab. 1 and for the servicer spacecraft those presented in Tab. 2.

In this dummy setup both spacecraft are situated in the same point in space, that is they have the same MOE and thus the ROE generated from the "ideal" MOE are all zero. In this way, the ROE generated with MOE containing RMS errors reflect nothing but the impact of those RMS errors. The ROE errors calculated for the example mission are summarized in Tab. 3. For the relative semi-major axis δa and the relative mean longitude $a\delta\lambda$ we also include the evolved error after 24 hours of propagation due to drag (i.e. $t - T_{End}$ = 24h in Eq. 2).

From Tab. 3 we find the ROE errors to decrease in general with the growth of the observation arc PTD and the growth of the number of tracking passes NTP. A partial exception from this tendency can be noticed in some elements, which may be attributed

to the corresponding irregularities in the calculated TIRA error characteristics caused by the limitedness of the tracking cases for any PTD/NTP configuration.

Table 3. Expected ROE errors (RMS) in 550 km altitude orbit.

PTD, NTP	δa [m]		$a\delta\lambda$ [m]		$a\delta e$ [m]	$a\delta i_x$ [m]	$a\delta i_y$ [m]
	T_{End}	T_{End}+24h	T_{End}	T_{End}+24h			
24h, 3	3.3	9.2	106.9	530.5	35.8	39.3	67.4
24h, 4	2.3	6.7	79.3	388.5	34.2	27.1	37.4
24h, 5	2.1	5.9	72.2	338.9	35.0	14.6	26.4
36h, 3	2.4	4.6	92.3	254.4	43.2	40.2	54.1
36h, 4	1.7	3.2	59.6	163.0	28.7	21.0	33.5
36h, 5	1.6	2.4	37.0	93.5	21.1	7.1	17.5
48h, 3	1.9	3.8	95.4	229.7	33.4	36.5	51.6
48h, 4	1.7	2.8	63.8	145.6	23.3	31.2	44.0
48h, 5	1.6	2.4	53.9	109.9	16.6	22.9	33.5
48h, 6	1.5	2.2	46.8	90.8	12.0	17.2	26.8
48h, 7	1.6	2.1	42.6	79.5	9.7	12.5	21.1

The more accurate knowledge of the ballistic coefficient as achieved for a 36 h observation arc compared to a 24 h arc (cf. Tab. 1) leads to a significant improvement in the prediction knowledge of both the relative semi-major axis and the relative mean longitude.

5. Conclusions

The following requirements on the radar-tracking are derived from the results of the CanX-2 campaign. Each Client radar-tracking campaign
- should cover a minimum of 24 hours of principal tracking duration (or 36 hours for a precise ballistic coefficient estimate),
- should comprise ascending and descending observations, and
- should include a minimum of 4 tracking passes.

Considering these requirements the ground-based orbit determination from Servicer GPS navigation data and Client radar tracking provides the Servicer-Client relative orbit elements in a 550 km example orbit with the following RMS errors:
- Relative mean longitude $a\delta\lambda$ (equivalent to the relative along-track separation) < 80 m at the end of the observation arc, or < 400 m after a 24 hour propagation,
- Relative semi-major axis a < 2.5 m, or < 7 m after a 24 hour propagation,
- Norm of the relative inclination vector $a\delta i$ (equivalent to the horizontal or normal separation) < 55 m, and
- Norm of the relative eccentricity vector $a\delta e$ (equivalent to the vertical or radial separation) < 35 m.

The achieved results demonstrate the potential of the proposed ground-based relative navigation concept for the far range approach of a debris removal or on-orbit servicing satellite to its target object. The provided RMS errors in the relative orbital elements are important parameters within the mission analysis and design phase. They are necessary, for example, to derive relative navigation sensor requirements or to design the formation geometry for the approach phase.

6. References

[1] Kirschner, M., Weigel, M., Kahle, R., Kahr, E., Choi, P., Letsch, K., Leushacke, L., "Orbit Precision Analysis of Small Man-made Space Objects in LEO Based on Radar Tracking Measurements", 23rd International Symposium on Spaceflight Dynamics, 29 Oct - 2 Nov 2012, Pasadena, CA, USA.

[2] Sarda, K., Eagleson, S., Caillibot, E.P., Grant, C., Kekez, D.D., Pranajaya, F., Zee, R.E., "Canadian Advanced Nanospace Experiment 2: Scientific and Technological Innovation on a Three-Kilogram Satellite", Acta Astronautica. 59:236-245, 2006.

[3] Spurmann, J., D'Amico, S., Sommer, J., "Ground-in-the-loop Relative Navigation for On-Orbit Servicing Missions in Low Earth Orbit", 4th International Conference on Spacecraft Formation Flying Missions & Technologies; 18-20 May 2011, St-Hubert, Quebec, Canada.

[4] D'Amico, S., Ardaens, J.-S., Gaias, G., Schlepp, B., Benninghoff, H., Tzschichholz, T., Karlsson, T., Jørgensen, J. L., "Flight Demonstration of Non-Cooperative Rendezvous using Optical Navigation", 23th International Symposium on Space Flight Dynamics, 29 Oct - 2 Nov 2012, Pasadena, CA, USA.

[5] Kahr, E., Montenbruck, O., O'Keefe, K., Skone, S., Urbanek, J., Bradbury, L., Fenton, Pat, F., "GPS Tracking of a Nanosatellite – The CanX-2 Flight Experience", 8th International ESA Conference on Guidance, Navigation & Control Systems, 5.-10. June 2011, Karlsbad, CZ.

[6] Wermuth, M., Hauschild, A., Montenbruck, O., Kahle, R., "TerraSAR-X precise orbit determination with real-time GPS ephemerides", Advances in Space Research 50, 549-559, (2012). DOI 10.1016/j.asr.2012.03.014.

[7] D'Amico, S., "Autonomous formation flying in low earth orbit", PhD thesis, Technical University of Delft (2010).